



Induction of Lung Cancer Cell Apoptosis through a p53 Pathway by [6]-Shogaol and Its Cysteine-Conjugated Metabolite M2

Renaud F. Warin, Huadong Chen, Dominique N. Soroka, Yingdong Zhu, and Shengmin Sang*

Center for Excellence in Post-Harvest Technologies, North Carolina Agricultural and Technical State University, North Carolina Research Campus, 500 Laureate Way, Kannapolis, North Carolina 28081, United States

ABSTRACT: Dietary chemoprevention of cancer offers the possibility to suppress or inhibit cancer growth before it develops into more advanced and lethal stages. To this end, identification of novel compounds and their mechanisms of action is constantly needed. In this study, we describe that a major component of dry ginger (*Zingiber officinalis*), [6]-shogaol (6S), can be quickly metabolized in A549 human lung cancer cell line. One of the resulting metabolites, the cysteine-conjugated 6S (M2), exhibits toxicity to cancer cells similar to the parent compound 6S, but is relatively less toxic toward normal cells than 6S. We further demonstrate that both compounds can cause cancer cell death by activating the mitochondrial apoptotic pathway. Our results show that the cancer cell toxicity is initiated by early modulation of glutathione (GSH) intracellular content. The subsequently generated oxidative stress activates a p53 pathway that ultimately leads to the release of mitochondria-associated apoptotic molecules such as cytochrome C, and cleaved caspases 3 and 9. In a xenograft nude mouse model, a dose of 30 mg/kg of 6S or M2 was able to significantly decrease tumor burden, without any associated toxicity to the animals. This effect was correlated with an induction of apoptosis and reduction of cell proliferation in the tumor tissues. Taken together, our results show that 6S metabolism is an integral part of its anticancer activities *in vitro* and *in vivo*. This allows us to characterize M2 as a novel compound with superior *in vivo* chemopreventive properties that targets similar anticancer mechanisms as 6S.

KEYWORDS: [6]-shogaol, cysteine conjugated metabolite, lung cancer, apoptosis, xenograft

INTRODUCTION

Cancer chemoprevention through dietary intervention has been the focus of intense interest because it can delay or avoid altogether the advent of cancer,¹ without the undesirable side effects traditionally associated with cancer treatments. Lung cancer is the most prevalent form of cancer-related death in the general population,² and a dietary chemopreventive strategy would be particularly effective because of its latency and the risk factors (such as smoking) associated with its development. Epidemiological studies showed that intake of fruits and vegetables can reduce lung cancer incidence.^{3,4} In other studies, this effect could be specifically correlated to carotenoids and flavonoids components with antioxidant activity.⁵ However, not all families of antioxidants can be correlated to a decreased risk of lung cancer,⁶ suggesting that the precise nature of the active compounds and the mechanism of action remain to be elucidated.

Ginger, the rhizome of *Zingiber officinalis*, has been widely used since ancient times for its medicinal properties, including an anticancer activity linked to its strong content in antioxidants.^{7–9} A recent human trial showed that intake of ginger can reduce the risk of colorectal cancer by reducing cell proliferation and apoptosis in a population of subjects at risk for this type of cancer.¹⁰ Several aromatic compounds with antioxidant properties have been isolated from ginger fractions.¹¹ Most recently, [6]-shogaol (6S), the major component of dried ginger, has garnered interest because of its superior anticancer activity and enhanced stability compared to its fresh extract counterpart, [6]-gingerol.¹² 6S mechanisms of action have been intensively studied *in vitro*, and it has been shown to modulate oxidative stress.^{13,14} This modulation has

been linked to the induction of apoptosis in Mahlavu hepatoma cancer cells¹³ or in COLO-205 human colon carcinoma cells,¹⁵ both cell lines being mutant for p53 expression. Induction of apoptosis was also possible in cells with normal expression of p53 such as the human colon cancer cell line HCT-116 or the lung cancer cell line H-1299.¹⁶ 6S was also shown to induce autophagy,¹⁷ cell cycle arrest,^{18,19} and inhibit cell invasion.^{20,21} In addition, it has been shown to inhibit angiogenesis²² and cancer cell proliferation in numerous cell lines.^{19,23–25} In A549 cells, 6S has been shown to induce cell death through autophagy and the activation of the AKT/mTOR pathway.¹⁷ Evidences of *in vivo* activity are limited, but 6S has been shown to reduce tumor burden and induce apoptosis through endoplasmic reticulum stress and activation of the PERK/eIF2 α pathway in a hepatocellular carcinoma cell xenograft model.²⁶ 6S is quickly metabolized by cells into several metabolites in humans²⁷ and in mice.¹⁶ Our lab recently demonstrated that one of these metabolites, the cysteine-conjugated 6S (M2), can modulate GSH levels in HCT-116 colon cancer cells and retain a bioactivity that is similar to the parent compound 6S in the nonsmall lung cancer cell line H-1299.^{14,28}

Our previous work established that M2 could potentially be a superior anticancer compound than 6S, due to its discriminatory properties.^{14,28} However, that data was obtained in nonsmall lung cancer cell line H-1299, which is a mildly

Received: December 13, 2013

Revised: January 19, 2014

Accepted: January 21, 2014

Published: January 21, 2014

aggressive type of lung cancer, and it is unclear whether these properties are conserved in more aggressive lung cancers such as small lung cancer cell types. Additionally, while several mechanisms of action of 6S have been identified, no study has considered the contribution of M2 to the mechanisms of action of 6S in cancer cells. Also, the mechanism of action of 6S *in vivo* remains largely unexplained, especially in light of its quick metabolism. In the present study, we test the hypothesis that the M2 metabolite can account for all or most of 6S bioactivity by activating similar molecular pathways in a determined sequence. We further correlate our findings on both compounds *in vivo* using a mouse xenograft model. Overall, this work describes for the first time that 6S and M2 can activate a similar cascade of pathways, ultimately leading to cancer cell apoptosis. It also demonstrates that the cysteine-conjugated metabolite has a superior *in vivo* cancer chemopreventive potential, in addition to its ability to discriminate between cancer and normal cells.

MATERIALS AND METHODS

Cell Culture and Reagents. A549 cells were cultured in F12K medium (Corning, NY) supplemented with 10% fetal bovine serum and 1% penicillin/streptomycin (Gemini Bio-Products, West Sacramento, CA). Protease and phosphatase inhibitor mix was from Thermo Scientific (Waltham, MA). Antibodies for Western blotting were from Cell Signaling (Danvers, MA). Protein concentrations were determined from cell lysates using a Pierce BCA kit (Thermo Fisher Scientific, Rockford, IL). BrdU (5-bromo-2-deoxyuridine) was from Sigma-Aldrich (St. Louis, MO). Apoptag plus Peroxydase In Situ Apoptosis Detection Kit was from Millipore (Billerica, MA), and the BrdU Immunohistochemistry Kit was from Chemicon International (Temecula, CA).

6S was purified from ginger extract in our laboratory.¹² M2 was synthesized in our laboratory, as previously reported.²⁹ HPLC-grade solvents and other reagents were obtained from VWR International (South Plainfield, NJ). LC/MS (liquid chromatography/mass spectrometry) grade solvents and other reagents were obtained from Thermo Fisher Scientific (Rockford, IL). Glutathione, sulfatase from *Aerobacter aerogenes*, and β -glucuronidase from *Helix aspersa* were obtained from Sigma Aldrich (St. Louis, MO).

Metabolism of 6S and M2 in A549 and IMR90 Cells. A549 or IMR90 cells (1.0×10^6) were plated in 6-well culture plates and allowed to attach for 24 h at 37 °C in 5% CO₂ incubator. 6S or M2 (in DMSO) was then added to culture media to reach a final concentration of 10 or 20 μ M, respectively. At different time points (0, 30, 1, 2, 4, 8 min, and 24 h), 190 μ L samples of supernatant were taken and transferred to vials containing 10 μ L of 0.2% acetic acid to stabilize 6S, M2, and their respective metabolites. To extract compounds from the culture media, an equal volume of acetonitrile was added to the supernatant samples and these mixtures were centrifuged. The supernatant was harvested and the samples were analyzed by HPLC-ECD as described by us previously.¹⁴

Determination of Cell Viability. A549 cell viability was determined by a 3-(4,5-dimethylthiazol-2-yl)-2,5-diphenyltetrazolium bromide (MTT) colorimetric assay.³⁰ A549 cells (6000 cells/well) were plated in 96-well microtiter plates and allowed to attach for 24 h at 37 °C and 5% CO₂. 6S or M2 (in DMSO) were added to cell culture medium to desired final concentrations (0–80 μ M; final DMSO concentrations for control and treatments were 0.1%). After the cells were cultured for 24 h, the medium was aspirated and the cells were treated with 2.41 mM MTT in fresh media. After incubation for 3 h at 37 °C, the medium containing MTT was removed, 100 μ L of DMSO was added to the wells, and the plates were shaken gently for an hour at room temperature. Absorbance values were derived from the plate reading at 550 nm on a Biotek Synergy 2 plate reader (Winooski, VT). The experiment was repeated independently to confirm the results.

Determination of Apoptosis. We used the Cell Death Detection ELISA (Enzyme-linked immunoabsorbant assay) Plus kit from Roche (Mannheim, Germany). A549 cells (10 000 cells/well) were plated in 96-well microtiter plates and allowed to attach for 24 h at 37 °C and 5% CO₂. 6S or M2 (in DMSO) was added to cell culture medium to desired final concentrations (10 or 20 μ M; final DMSO concentration for control and treatments was 0.1%). After 24 h, the microplate was centrifuged for 10 min at 1200 rpm, and the supernatant was removed. Then, 200 μ L of the lysis buffer was added in each well and the microplate was incubated for 30 min at room temperature. The plate was then centrifuged for 10 min at 1200 rpm and 20 μ L of the supernatant was transferred to streptavidin-coated microwells. ELISA assay was performed according to manufacturer's instruction. Absorbance in each well was measured at 405 nm in absorbance units (AU), and the enrichment factor (EF) in small nucleosomes was calculated with the formula $EF = AU_{(treated)} / AU_{(DMSO)}$. The experiment was repeated independently to confirm the results.

Intracellular Glutathione (GSH) Measurement. The total GSH content was measured using a HT Glutathione Assay kit (Trevigen, Gaithersburg, MD). Briefly, A549 cells were plated in 60 \times 15 mm culture plates and were allowed to attach overnight at 37 °C. Cells were treated with 10 μ M M2 and incubated for 0, 2, 4, 8, or 24 h. Cells were harvested and proteins were precipitated with 5% (w/v) metaphosphoric acid. Samples were then processed following the manufacturer's instructions. The measurement of the absorbance of 5-thio-2-nitrobenzoic acid (TNB) at 405 nm was used to quantify glutathione levels in each sample, which was then compared to the standard curve and corrected for protein concentration. The experiment was repeated independently to confirm the results.

For measurement of oxidized glutathione (Glutathione Disulfide or GSSG), samples and GSSG standards were treated with 2 M 4-vinylpyridine (1 μ L/50 μ L sample) at room temperature for 1 h. 4-Vinylpyridine (Sigma Aldrich, St. Louis, MO) blocks free thiols present in the reaction, consequentially blocking the formation of new GSSG by GSH. The 2 M solution was freshly prepared by diluting 4-vinylpyridine in ethanol in a ratio of approximately 1:3:6. After incubation, samples were processed using the Trevigen kit's protocol and absorbance was measured at 405 nm as described above.

The quantity of reduced cellular glutathione (or GSH) is obtained by subtracting the oxidized samples values from the total glutathione values or: $GSH_{(reduced)} = GSH_{(total)} - GSSG_{(oxidized)}$. Ratios of reduced to oxidized glutathione are shown to further represent cellular redox status after treatment with 6S or M2. The experiment was repeated independently to confirm the results.

Western Blotting. Cell extracts were prepared by incubating cells for 5 min on ice with RIPA (Radio-Immunoprecipitation Assay) buffer (Thermo Fisher Scientific, Rockford, IL) supplemented with a protease and phosphatase inhibitor mix. Cell lysate was then centrifuged at 13 000 rpm at 4 °C for 20 min, and supernatant was harvested for Western blot analysis. Briefly, 30–60 μ g of protein extract was separated on a 10–16% polyacrylamide gel and transferred on PVDF (polyvinylidene difluoride) membrane (Biorad, Hercules, CA). Membrane was blocked using a 1% casein solution in Tris-buffered saline-Tween 20 (TBS-T). Primary rabbit antibodies were diluted in blocking solution and incubated with the membrane overnight at 4 °C. After the membrane was washed with 3 changes of TBS-T, secondary Horse Radish Peroxydase (HRP)-conjugated anti-rabbit antibody was diluted 1:3000 in blocking solution and incubated with PVDF membrane for 1 h at room temperature. Signal was then revealed using FEMTO chemoluminescent substrate (Thermo Scientific, Waltham, MA) and by exposing the membrane to photosensitive photographic films for various times. Films were developed using a SRX-101A Konica Minolta developer (Tokyo, Japan). The experiment was repeated independently twice to confirm the results. Fold-induction of proteins was calculated by normalizing the band of interest to the loading control (β -actin), and this adjusted intensity was compared to the control (DMSO) sample.

GSH Rescue Assay. A549 cells were plated on 60 mm culture dishes, at 0.5×10^6 density. After 24 h, DMSO, 6S or M2 (10, 20, 40, 80, 120 μ M) were added to the cells and incubated with or without the

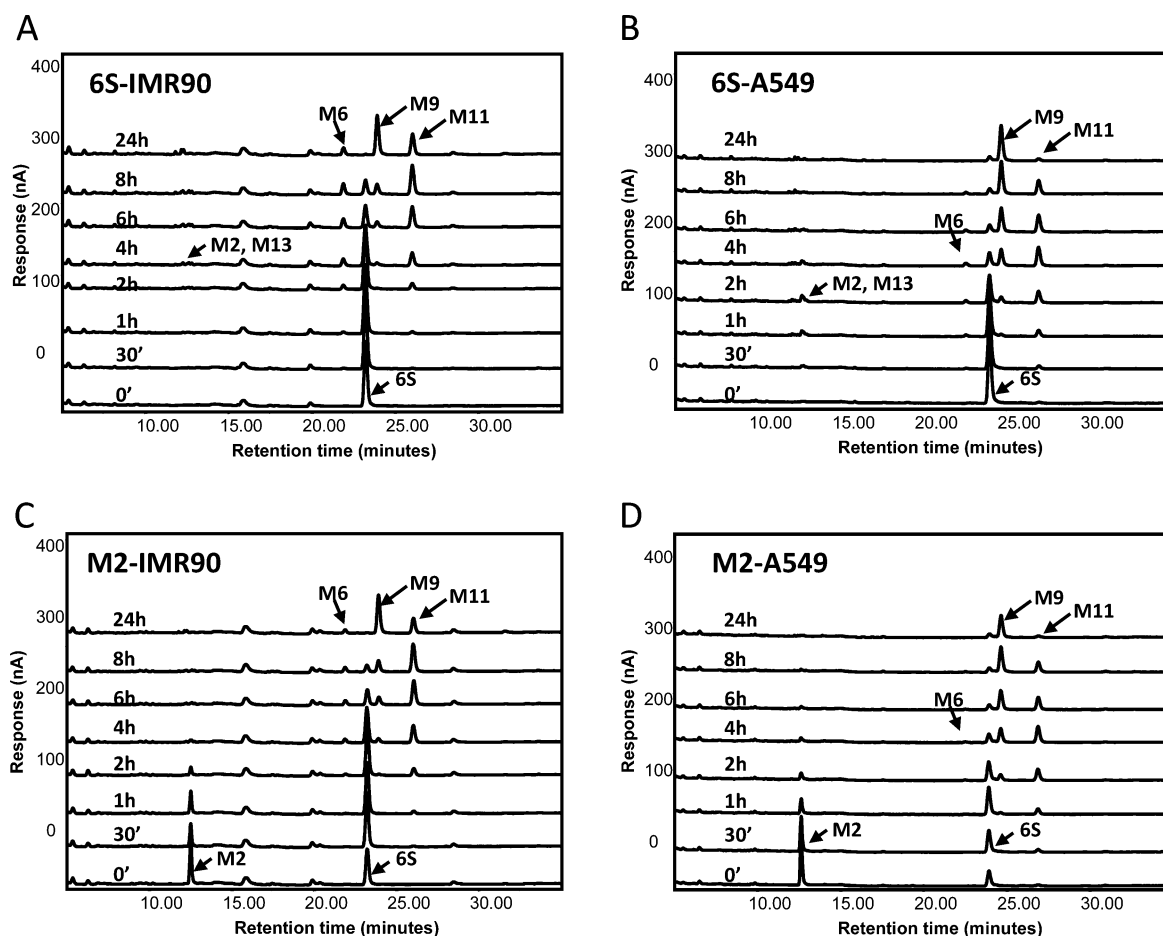


Figure 1. HPLC metabolic profile of IMR90 (A and C) or A549 (B and D) cells exposed to 10 μ M of 6S (A and B) or M2 (C and D) after 0, 0.5, 1, 2, 4, 6, 8, and 24 h.

addition of 5 mM GSH in the culture media. After 24 h, toxicity was assessed using the MTT assay and using the method described above. The experiment was repeated independently to confirm the results.

Animal Experiments. Experiments with mice were carried out according to protocol approved by the Institutional Review Board for the Animal Care and Facilities Committee at North Carolina Research Campus and North Carolina Agricultural and Technical State University. Nu/J nude mice were obtained from Jackson Laboratories (Bar Harbor, ME). Animals were randomized into 4 groups. A549 cells (5×10^6 cells) were implanted in both flanks of 8-weeks old Nu/J mice. One week after implantation, animals were given 100 μ L of the following treatments through oral gavage 5 times/week: DMSO 0.25 mL/kg (control; $n = 4$); 6S 10 mg/kg ($n = 4$); 6S 30 mg/kg ($n = 4$) or M2 30 mg/kg ($n = 5$). Compounds were diluted in a solution of 5% DMSO in corn oil. Animal body weight and tumor volume were recorded for the duration of the experiment. Tumor volume was calculated by measuring the length and width of the tumors using a digital caliper and using the formula $(\text{Length} \times \text{Width}^2)/2$. One hour before sacrifice, mice were given one last treatment dose as well as one intraperitoneal injection of BrdU (7.5 mg/kg in 100 μ L PBS). After 7 weeks, tumor tissues were harvested and weighed. A portion of the tumors was snap frozen in liquid nitrogen and another portion was placed in a histology cassette and immersed in formalin solution.

Immunohistochemistry. Formalin-fixed tissues were sent to Precision Histology Lab (Oklahoma City, OK) for embedding in paraffin blocks. Paraffin blocks were then processed into 3–4 μ m sections that were then put on microscope slides. Sections were then deparaffinized by using a succession of 3 baths of xylene (5 min each), 2 baths of absolute ethanol (5 min each), 95% ethanol for 3 min, 70% ethanol for 3 min, and rinsed in PBS. Immunostaining with TUNEL (terminal deoxynucleotidyl transferase dUTP nick end labeling) and

BrdU staining kits was performed following manufacturer's recommendation. For staining quantification, sequential high-power field pictures of tumors were taken (10 pictures per tumor) using an A1 Zeiss microscope (Oberkochen, Germany). Images were processed using the Image J software,^{31,32} which was used to count positive, brown-colored cells in each field. Average number per tumor was calculated by averaging the number obtained for each field, and the average number of positive cells per group was obtained by averaging the values of each tumor belonging to the experimental group.

Statistics. Statistics were calculated using either a two-tailed Student *t* test, or ANOVA followed by Bonferroni's post-test. Results were considered significant when $p < 0.05$.

RESULTS

6S and M2 Are Similarly Metabolized by IMR90 and A549 Cells. We recently published that 6S is metabolized in cancer cells and that its bioactivity -i.e. selective toxicity- can be attributed to some of its metabolites, notably M2.^{28,29} For this study, we first needed to determine if 6S or M2 are similarly metabolized in our model of small cell lung cancer A549 human cells as well as in IMR90 human normal lung cells. After exposing A549 or IMR90 cells to 10 μ M of 6S or M2, we analyzed the metabolic profiles obtained from the culture supernatants at different time points using HPLC-ECD. We confirmed that 6S is metabolized by IMR90 or A549 cells (Figure 1, panel A or B, respectively), with an initial conversion into mostly the metabolites named M2, M13 and M11, while in later time points, most of 6S has been metabolized into M9.²⁹ The structures of all metabolites were confirmed using LC/MS

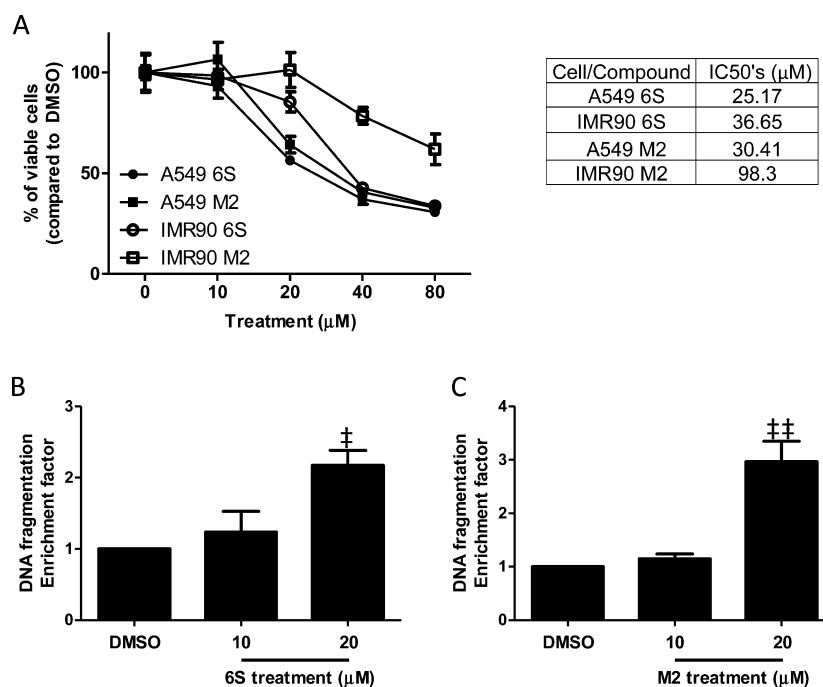


Figure 2. (A) 6S and M2 toxicity in A549 cancer cells and IMR90 normal lung cells using MTT assay, with the corresponding IC₅₀ values on the right side table. (B) Apoptosis measured by ELISA assay in A549 cells after 24 h treatment with 10 or 20 μM of 6S. (C) Apoptosis measured by ELISA assay in A549 cells after 24 h treatment with 10 or 20 μM of M2. Bars, SEM; [‡], $p < 0.05$; ^{‡‡}, $p < 0.01$ using one-way ANOVA followed by Bonferroni's post-test.

analysis (data not shown). As initially reported in HCT-116 and H-1299 cells,²⁸ M2 metabolism in IMR90 (Figure 1C) or A549 cells (Figure 1D) was also characterized by an initial conversion of this cysteine-conjugated metabolite back into 6S, which is then metabolized in a similar pattern than described above for 6S. These results show that normal lung IMR90 and lung cancer A549 cells can quickly metabolize 6S and M2 in a similar pattern, which correlates with the observations in other cell models.²⁸

M2 Toxicity Can Selectively Target Cancer Cells Compared to 6S. Our results show that M2 can quickly revert back to 6S native form when metabolized by A549 cells. We wanted to determine if that reversion led to a distinct bioactivity or if the parent compound and M2 shared the same bioactivity. We used an MTT assay to compare the bioactivity of 6S and M2 in A549 cells as well as in IMR90 human, noncancerous lung cells. The results are summarized in Figure 2A. When treated with increased concentration of 6S or M2, we detected an increase in toxicity in A549 cells with IC₅₀'s of 25.2 and 30.4 μM , respectively. In IMR90 cells, the IC₅₀ was 36.6 and 98.3 μM for 6S and M2, respectively. In other words, in normal cells the IC₅₀ value was 45.6% higher for 6S and 223.2% higher for M2 when compared to A549 cells. These results show that 6S and M2 exert similar toxicity toward A549 cells. However, M2 toxicity is greatly diminished against noncancerous cells compared to that of 6S.

6S and M2 Activate the Apoptosis and p53 Pathways. Since our results show that 6S and M2 are bioactive against A549 cancer cells, we tried to determine the potential mechanisms of activation by looking at apoptosis, since it is one of the major pathways that can be specifically activated by the exposure to environmental stressors, and that ultimately leads to cell death. We used an ELISA assay that quantified the release of cytoplasmic histone-associated DNA fragments in

A549 cells exposed to 6S or M2 for 24 h. Figure 2B shows that after 24 h these apoptotic markers were significantly higher (enrichment factor of 2.2) for cells treated with 20 μM of 6S. We also detected a significant increase in apoptotic markers (about 3-fold enrichment) after treatment with 20 μM M2 (Figure 2C).

To confirm these results, we performed Western blot analysis on extracts of A549 cells treated with 20 or 40 μM of 6S or M2 for 2 or 24 h. The results are summarized in Figure 3. For both concentrations of 6S or M2, we found that the pro-apoptotic markers cytochrome C, cleaved caspases 3 and 9 were markedly elevated after 2 h. Only cleaved caspases 3 and 9 levels remained elevated after 24 h, especially at the 40 μM concentration. Consistently, we could detect a small increase of caspases 3 and 9 after 2 h of exposure, and these levels were lower after 24 h. Markers of the mitochondrial apoptotic pathway Bax, Bak and Bcl-2 were all slightly elevated after 2 h of exposure to the test compound, but their levels were close to that of DMSO-treated cells after 24 h.

Since we could not detect any meaningful changes in the mitochondrial apoptotic pathway associated with the release of cytochrome C and subsequent caspase cascade activation,³³ we looked into the p53 pathway since it is responsive to oxidative stress and capable of triggering apoptosis.³⁴ Indeed, our results showed an increase in p53 levels after 2 and 24 h treatment with 6S or M2. It correlated with an increase of one of its downstream targets PUMA (p53 upregulated modulator of apoptosis), which was most evident after 24 h (Figure 3, top lines). These results show that both 6S and M2 can activate the p53 and the apoptosis pathways.

Excess GSH Can Rescue A549 Cells from 6S and M2 Toxicity and Suppress p53 Activation. Recent studies in our group showed that 6S can modulate GSH levels in HCT-116 colon cancer cells,¹⁴ and we wanted to determine if that

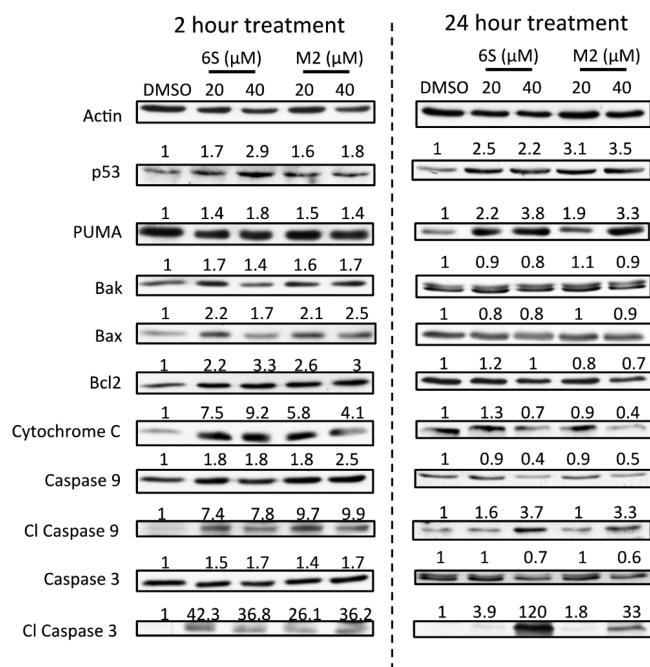


Figure 3. Western blot analysis of cell extracts after treatment with DMSO (control), 20 or 40 μM of 6S or M2 for 2 and 24 h. Markers are indicated on the left. Fold induction for each marker compared to DMSO is indicated over the corresponding line and was calculated as indicated in Material and Methods section.

effect was also present in the A549 small lung cancer cells model using 6S and M2. Figure 4A,B shows that GSH levels are significantly depleted as early as 2 h after exposure to 10 μM of 6S or M2. This depletion further continues after 4 h. After 8 h, GSH levels were still significantly lower in 6S treated cells, and

significantly higher in M2 treated cells. After 24 h, GSH levels were significantly increased after exposure to both compounds compared to baseline. While changes of GSH levels are not as large as those of 6S in the case of M2, it is nonetheless significant for all tested time points.

When cells are exposed to increased levels of oxidative stress, GSSG will accumulate and the ratio of GSH to GSSG will decrease.³⁵ The results of a GSH/GSSG assay are presented in Figures 4C (for 6S) and 4D (for M2). This experiment shows that after 2 h the GSH/GSSG ratio is significantly lower for 6S-treated (10 μM) cells but not for M2-treated (10 μM) cells. After 4 h of exposure to 6S or M2, the GSH/GSSG ratio is significantly lower and after 24 h of exposure it is significantly higher. Collectively, these results show that both 6S and M2 can deplete GSH levels and induce oxidative stress in A549 cells in a similar fashion.

We demonstrated that 6S and M2 can modify GSH levels, but it is unclear whether this effect can be directly linked to their apoptotic activity. We wanted to verify the link between GSH modulation and apoptosis by conducting a GSH rescue assay in which excess GSH in the culture medium essentially prevented any fluctuation in GSH level after treatment with the test compounds. Excess GSH in the culture media completely rescued A549 cells from both 6S and M2 toxicity, with modified IC_{50} 's over 80 μM (Figure 5A). Western blot analysis showed that in the presence of excess GSH, there was no change in p53 expression in the 24 h extracts of cells treated with 40 μM 6S or M2 (Figure 5B). These results show that the changes in GSH levels induced by both 6S and M2 in A549 cells are necessary to induce toxicity and the p53 pathway.

The p53 Pathway Is Involved in 6S and M2-induced Toxicity and Apoptosis. We further investigated the involvement of p53 pathway in 6S or M2-induced toxicity and apoptosis by using the p53-specific inhibitor pifithrin μ

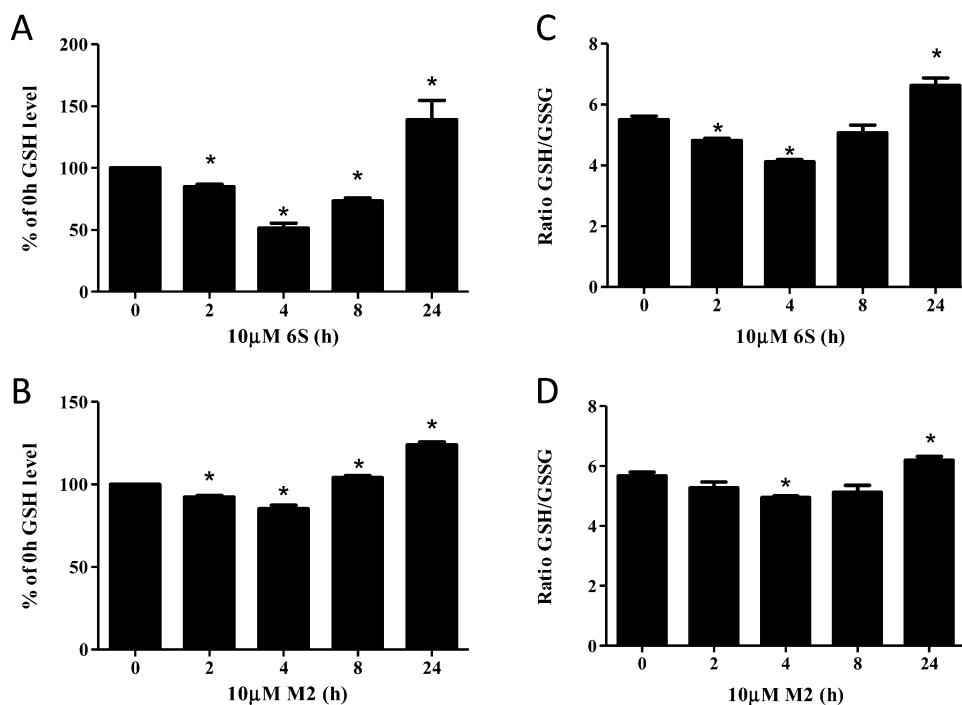


Figure 4. (A) Intracellular total GSH levels and (C) GSH/GSSG ratio in A549 cells treated with 10 μM of 6S for 0, 2, 4, 8, and 24 h. $[\text{GSH}]_{\text{DMSO } 0\text{h}} = 43.37 \pm 5.85 \text{ nmol/mg}$. (B) Intracellular total GSH levels and (D) GSH/GSSG ratio in A549 treated with 10 μM of M2 for 0, 2, 4, 8, and 24 h. $[\text{GSH}]_{\text{DMSO } 0\text{h}} = 44.46 \pm 5.16 \text{ nmol/mg}$. Bars, SEM; *, $p < 0.05$ by Student t test.

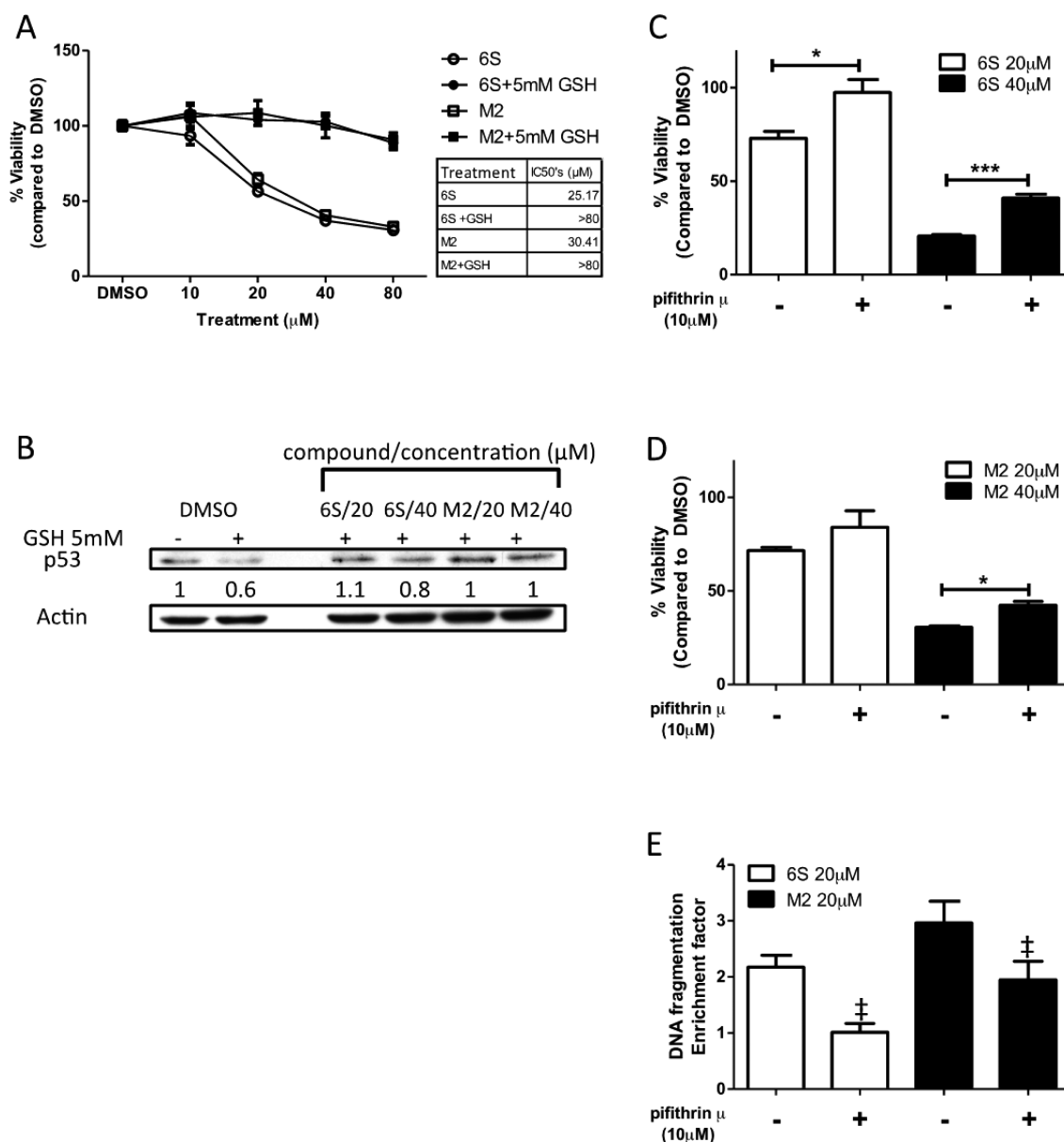


Figure 5. (A) GSH rescue assay in A549 cells. Cells were treated for 24 h with 0, 10, 20, 40, or 80 μ M of 6S or M2 in the presence or absence of 5 mM GSH. The associated table indicates the IC₅₀ values for each treatment. (B) Western blotting analysis of cell extracts treated with DMSO, 20 or 40 μ M of 6S or M2 for 24 h with or without 5 mM of GSH. Fold induction for each marker compared to DMSO is indicated under the corresponding line and was calculated as indicated in Material and Methods section. (C) Effect of pft treatment on A549 cell death after treatment with 20 or 40 μ M of 6S for 24 h. (D) Effect of pft treatment on A549 cell death after treatment with 20 or 40 μ M of M2 for 24 h. (E) Effect of pft treatment on A549 cell apoptosis after treatment with 20 μ M of 6S or M2 for 24 h. Bars, SEM; *, $p < 0.05$; ***, $p < 0.001$ using a paired Student's t test; ‡, $p < 0.05$ using one-way ANOVA followed by Bonferroni's post-test.

(pft). This inhibitor can block the direct interaction and mitochondrial relocation of p53 with members of the Bcl-2 family.³⁷

Treatment of A549 cells with pft in addition to 6S was very effective in reducing the toxic effect of both 6S (Figure 5C) and M2 (Figure 5D). When treated with 20 μ M of 6S or M2 for 24 h, the percentage of viable cells was close to 100% for 6S and 84.2% for M2. Without pft to block p53 interaction with Bcl-2 family members, the percentage of viable cells was only around 72% in both cases. This effect was also observed at a higher dose of compound (40 μ M). In the case of 6S, the percentage of viable cells was significantly higher (20.6% of viable cells without pft and 41% of viable cells with pft). For 40 μ M M2, the effect was similar, with 30.6% of viable cells without pft and

42.4% of viable cells with pft. These results show that interfering with p53 signaling can at least partially rescue cells from 6S and M2-induced toxicity.

Since pft directly interferes with p53 signaling toward the mitochondria, we also tried to determine the effect of pft on apoptosis induction in A549 cells. For this experiment, a 20 μ M dose was used since we established it to be the most effective dose for this assay (Figure 3B,C). The treatment with pft reduces the enrichment factor in small nucleosomes by a factor of 1 for both 6S and M2 (Figure 5E): in the case of 6S, the presence of pft significantly returned the enrichment factor to baseline (about 1), while in the case of M2, the enrichment factor is significantly down to 2 with pft from 3 without pft. Altogether these results show that 6S and M2 induce cell

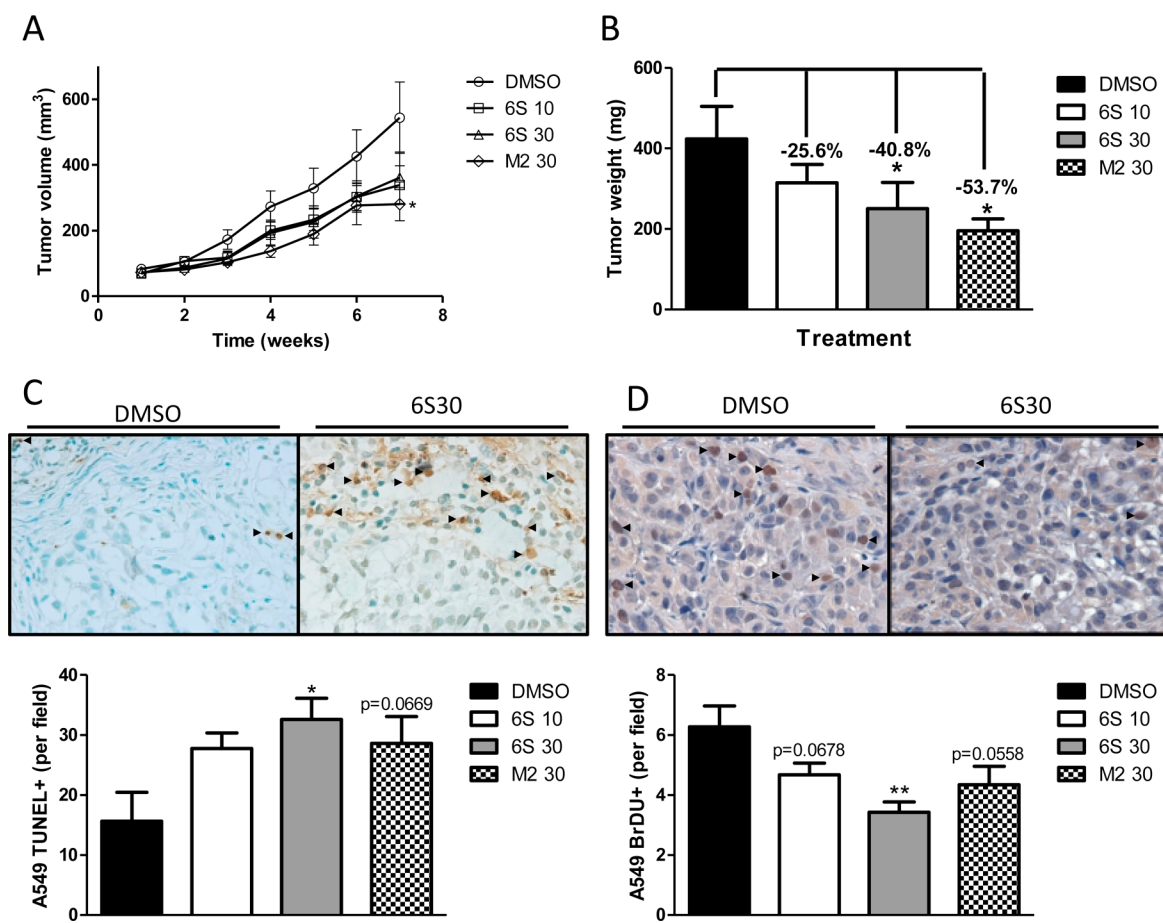


Figure 6. Xenograft experiment using A549 cells in nude mice. Animals were oral-gavaged 5X/week for 7 weeks with DMSO (control), 10 mg 6S/kg body wt (6S 10), 30 mg 6S/kg body wt (6S 30), or 30 mg M2/kg body wt (M2 30). (A) Changes in tumor volume (in mm³) after 1-, 2-, 3-, 4-, 5-, 6-, and 7-week treatment with test compounds. (B) Wet tumor weight after 7-week treatment. (C) TUNEL immunostaining of 3–4 μ m sections of tumor tissue. Representative picture from the DMSO and the 30 mg 6S/kg body wt (6S30) groups are showed on the top, and TUNEL-positive apoptotic cell quantification is presented at the bottom. (D) BrdU immunostaining of 3–4 μ m sections of tumor tissue. Representative picture from the DMSO and the 30 mg 6S/kg body wt (6S 30) group are showed on the top, and BrdU-positive cell quantification is presented at the bottom. Bars, SEM; *, $p < 0.05$; **, $p < 0.01$ using unpaired Student's t test.

apoptosis through the modulation of GSH levels and the activation of a p53 pathway.

6S and M2 Can Reduce Tumor Burden in Nu/J Mice. It is always uncertain how an observed anticancer bioactivity of a given natural compound translates *in vivo*, mainly due to the fast turnover and degradation of the compounds.^{16,27} To ascertain the bioactivity of 6S and M2 *in vivo*, we studied their effect on the development of A549 tumors in a mouse xenograft model.

Exposure of animals to a daily oral gavage for up to 7 weeks did not induce any significant changes in body weight between groups (data not shown). Tumor volume in the control group grew exponentially, tumors from the groups receiving 6S 10 mg/kg, 6S 30 mg/kg or M2 30 mg/kg grew markedly slower, with tumors from the M2 group being significantly different by week 7 (Figure 6A). After 7 weeks, tumor weight was significantly lower in both 6S 30 mg/kg (minus 40.8% compared to DMSO-treated control) and M2 30 mg/kg (minus 53.7% compared to DMSO-treated control). Tumor weight was also markedly lower in the 6S 10 mg/kg group (minus 25.6%), albeit not significantly (Figure 6B). Taken altogether, both treatments were sufficient to lower the tumor burden of A549 engrafted cells at a 30 mg/kg body weight. Interestingly M2 appeared to be the most active compound *in*

in vivo, albeit not significantly when compared to the 6S 30 mg/kg treatment.

6S and M2 Induce Apoptosis and Reduce Cell Proliferation in A549 Xenografts. Next we sought to investigate the mechanisms by which 6S and M2 can reduce tumor burden in A549 xenografts tissues. TUNEL staining of tumor tissues (Figure 6C) showed a marked increase of apoptotic bodies in the animals treated with 6S 10 mg/kg body wt (27.8 TUNEL+ cells/field) compared to control (about 15.5 TUNEL+ cells/field). This trend became significant in the tumors from animals treated with 6S 30 mg/kg, with an average of 32.6 TUNEL+ cells/field. In the case of the animals treated with M2 30 mg/kg, we also observed the same trend (28.6 TUNEL+ cells/field) that was very close to being significant ($p = 0.0669$). BrdU staining of tumor tissues (Figure 6D) showed a significant reduction of cell proliferation in the animals treated with 6S 30 mg/kg body wt (3.4 BrdU+ cells/field) compared to control (about 6.3 BrdU+ cells/field). We also detected a marked reduction of cell proliferation in the 6S 10 mg/kg group (4.7 BrdU+ cells/field) that was very close to significance ($p = 0.0678$ by unpaired t test compared to control). While there was also a slight decrease in the M2 30 mg/kg group (4.3 BrdU+ cells/field), it was also very close to significance ($p = 0.0558$ by unpaired t test compared to control). These results

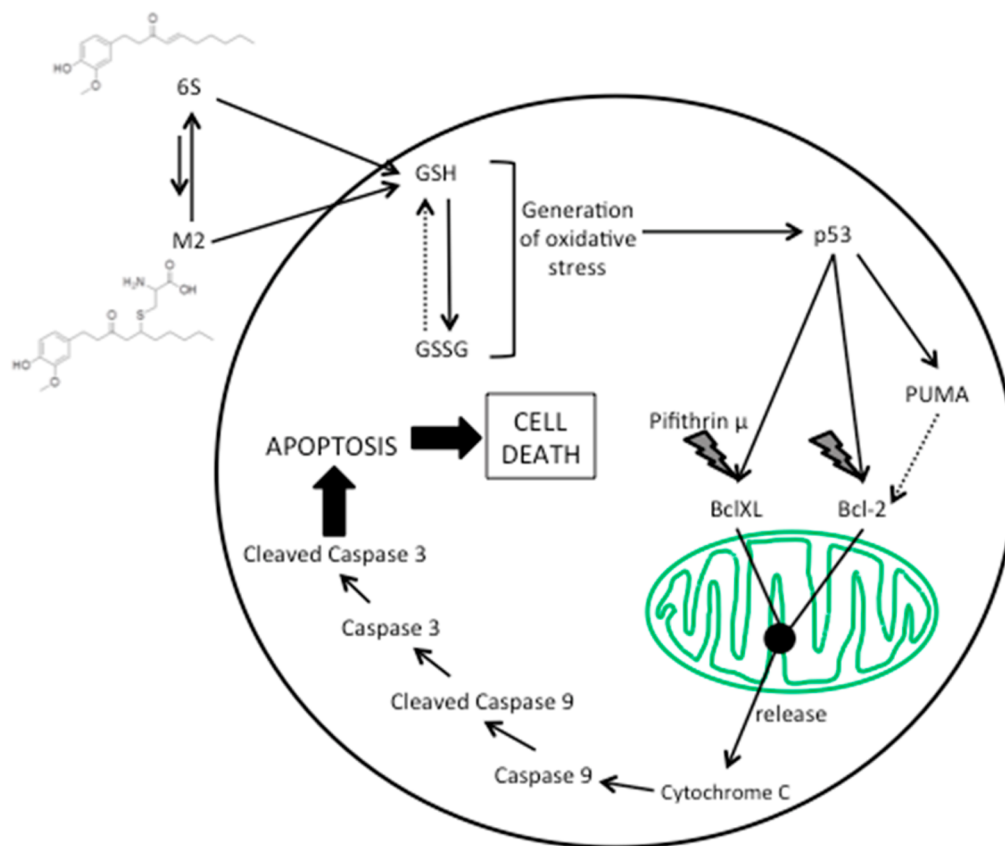


Figure 7. Schematic representation of the proposed mechanism of apoptosis activation in A549 cells by 6S and its cysteine-conjugated metabolite M2. Dotted arrows: possible interactions. Plain arrows: proposed interactions.

show that the reduction in tumor burden *in vivo* can be correlated to the induction of apoptosis for 6S and M2. In the case of 6S, it can also be associated to others molecular mechanisms such as cell proliferation.

DISCUSSION

Dietary intervention is a well-accepted mean of reducing cancer events. Cohort studies show that increased intake of fruits, vegetables and spices are indeed inversely correlated with the risk of various cancers.^{3,4} While a full explanation for these observations is still heavily investigated, there is no doubt that dietary compounds can have long-term health benefits in terms of cancer prevention despite their fast metabolisms. Our lab showed that 6S, the major component of dried ginger, can be rapidly metabolized in colon and nonsmall cell lung cancer cells.²⁸ This proved to be also true in the human lung cancer cell model A549 (Figure 1), which is of the more aggressive type of lung cancer.

We initially assessed the bioactivity of 6S and M2 in A549 using an MTT assay. While both compounds displayed a significant toxicity toward cancer cells, it was remarkable that M2 was significantly less toxic toward noncancerous cells. 6S did not possess this property, suggesting that the cysteine-conjugation of 6S allowed discrimination between cancerous and normal human lung cells. This result validated its usefulness as a superior anticancer compound compared to 6S, and justified further investigation of M2. While the noncancerous lung cell line IMR-90 is from a different embryonic origin than A549, there is no perfect normal cell

line that is currently available *in vitro*. In consequence, further *in vivo* toxicity study of 6S and M2 is warranted.

We then tried to gain insight into the mechanism of action of both compounds. Our laboratory previously demonstrated in others models that 6S and several other metabolites were able to trigger apoptosis,^{16,29} a mechanism of programmed cell death that is often impaired in cancer cells. We determined that 6S and its metabolite M2 could also activate the apoptosis pathway in A549 cells. This was demonstrated by the detection of cytoplasmic histone-associated-DNA-fragments in A549 cells upon treatment with 6S or M2 for 24 h. Notably, we demonstrated that while the IC_{50} of M2 is higher than 6S, its capacity to specifically induce apoptosis was superior (as shown in Figure 2). Additionally, we showed the activation of the apoptosis pathway by demonstrating the modulation of final apoptotic markers such as cytochrome C, caspases 3 and 9 and their cleaved isoforms. Caspase 9 was also slightly elevated after 2 h of exposure, but it could be the result of newly synthesized protein to reinforce the already activated apoptotic pathway. These markers are part of the mitochondrial apoptotic pathways, but interestingly the traditionally associated markers of the Bcl-2 family (Bak, Bax) were not affected. Bcl-2 showed a small increase after 2 h, but the increase did not appear to be concentration-dependent and was very modest compared to the others markers, which suggest a very limited influence. On the other hand, we were able to detect a very early increase in p53 and PUMA, two major actors in the transmission of cellular changes such as (but not limited to) oxidative stress. Indeed, as was previously described in other cell lines, treatment of A549 cells with 6S and M2 led to a clear disturbance in GSH

homeostasis, which would explain the generation of oxidative stress. This disturbance has been observed before and can be explained by the property of dietary electrophiles to activate the transcription factor Nrf2:³⁸ after the initial depletion of GSH to detoxify electrophiles compounds, the cellular GSH levels can be restored and even enhanced by the subsequent Nrf2-mediated signal and GSSG recycling. This mechanism exists in order to maintain cell equilibrium, and rescuing it from oxidative damage or others carcinogens. However, GSH variation, if too great, can also be interpreted by cellular components as irreparable damage, which requires the cell to engage into the apoptotic pathway.

The next question was to determine the mechanism of transition from oxidative stress to apoptosis. p53 is known to be able to trigger apoptosis through interaction with members of the Bcl-2 family such as Bax, Bcl-2 or Bcl-XL to trigger apoptosis without modifying their level of transcription.^{39,40} Using the chemical inhibitor pft, we show here that the interaction between Bcl-2 or Bcl-XL and p53 might be disrupted, as evidenced by a reduced toxicity of both 6S and M2 (Figure 5C,D), as well as the induction of apoptosis (Figure 5E). It has been reported that pft is also a known inhibitor of hsp70.³⁶ Whether hsp70 is also a target of 6S or M2 is a topic for future study. Nevertheless, our results suggest a direct relationship between the propagation of a mitochondrial apoptotic signal and an induction of p53 expression, which could explain the lack of variation in the Bcl-2 family markers expression. The proposed pathway of cancer cell apoptosis induction is summarized in Figure 7. It is interesting to note, however, that while apoptosis could be almost completely abolished by pft in lower doses of compounds, the cell viability could never be completely rescued. We also observed a marked increase in PUMA expression, especially after 24 h of exposure to both 6S and M2 (Figure 3). PUMA is another molecule that can mediate the p53 apoptotic message through its interaction with members of the Bcl-2 family.⁴¹ This suggests that apoptosis is in part accountable for the death of A549 cells, and that multiple mechanisms inducing apoptosis and/or toxicity in cancer cell might be acting together.

While we determined that both 6S and its metabolite M2 can trigger similar biological responses and mechanisms in A549 cells, it was unclear if this would still be true *in vivo*. This was a concern especially when taking into account the short half-life of these compounds due to their quick metabolisms, as our previous studies reported.¹⁴ To this end, we carried out a xenograft experiment where A549 tumor growth was significantly delayed by both 6S and M2. Additionally, M2-treated animals showed a further reduction in tumor burden compared to the animals treated with 6S at an equivalent dose of 30 mg/kg body wt (Figure 6B). As demonstrated by TUNEL staining of tumor tissues, 6S could significantly induce apoptosis *in vivo*, while M2 was very close to also having a significant effect. However, there was still a clear trend and it is probable that the number of animals used was not sufficient and that an increased number would allow for the detection of a significant induction of apoptosis even by M2 (Figure 6C). We also demonstrated that both 6S and M2 can decrease cell proliferation (Figure 6D). Similarly to what we observed by TUNEL staining, only 6S at the higher dose was shown to have a significant effect, while M2 was close to having a significant effect. As described above, this is expected since we showed that blocking of the apoptotic pathway through chemical methods *in vitro* could only partially rescue cells from the toxicity of 6S and

M2. Similarly, the percentage of apoptotic cells detected by ELISA could not be entirely restored to DMSO (control)-treated levels, especially at the higher concentration (40 μ M) of the compounds, when treated with pft. The fact that the exposure to our compounds results in an increase of the multiacting molecule p53 can also explain the activation of multiples pathways. The p53 pathway has been demonstrated to have multiple effects, and is a major regulator of the cell cycle.⁴² In this light, it is not surprising that cell proliferation would be affected by the exposure to compounds that can increase p53 expression. It is particularly interesting in terms of cancer prevention since p53 expression is lost in most late-stage cancers but can still be active in early stage cancers or even aggressive cancers, such as in A549 cells. 6S and its metabolites could exert their activity in an optimal manner in these conditions, while M2 could also exert this activity and being harmless against normal cells.

Altogether, this study shows that the traditional model of bioactivity by natural compounds can be challenged and that the products of degradation of the parent compound can be responsible for the observed bioactivity. This would also explain how dietary compounds can exert a long-term effect despite being quickly metabolized. Finally, there is evidence that drug conjugation using cysteine can be an effective tool to deliver drugs to its target, as in the case of antibody-drug conjugates.^{43,44} Our lab previously suggested that M2 could act as a carrier for 6S to prolong or enhance its activity,²⁸ and the current study clearly reinforces this hypothesis. The cysteine group can be hydrolyzed out of M2 to form 6S in both A549 human lung cancer cells and IMR90 human normal lung cells. It appears that natural modifications of dietary compounds through metabolism, such as cysteine addition, can be a fertile source for the discovery of novel bioactive molecules and the identification of novel targets and strategies for cancer prevention and treatment.

AUTHOR INFORMATION

Corresponding Author

*Address: Center for Excellence in Post-Harvest Technologies, North Carolina Agricultural and Technical State University, North Carolina Research Campus, 500 Laureate Way, Kannapolis, NC 28081, USA. Tel: +1 704-250-5710. Fax: +1 704-250-5709. E-mail: ssang@ncat.edu.

Funding

Funding for this investigation was partially provided by grants CA138277 (S. Sang) from the National Cancer Institute and CA138277S1 (S. Sang) from National Cancer Institute and Office of Dietary Supplement of National Institutes of Health.

Notes

The authors declare no competing financial interest.

REFERENCES

- (1) Greenwald, P.; Nixon, D. W.; Malone, W. F.; Kelloff, G. J.; Stern, H. R.; Witkin, K. M. Concepts in cancer chemoprevention research. *Cancer* **1990**, *65*, 1483–1490.
- (2) American Cancer Society *Cancer Facts and Figures 2013*; ACS Annual Reports; American Cancer Society: Atlanta, GA, 2013.
- (3) Verhoeven, D. T.; Goldbohm, R. A.; van Poppel, G.; Verhagen, H.; van den Brandt, P. A. Epidemiological studies on brassica vegetables and cancer risk. *Cancer Epidemiol., Biomarkers Prev.* **1996**, *5*, 733–748.
- (4) Kolonel, L. N.; Hankin, J. H.; Whittemore, A. S.; Wu, A. H.; Gallagher, R. P.; Wilkens, L. R.; John, E. M.; Howe, G. R.; Dreon, D.

M.; West, D. W.; Paffenbarger, R. S., Jr. Vegetables, fruits, legumes and prostate cancer: a multiethnic case-control study. *Cancer Epidemiol., Biomarkers Prev.* **2000**, *9*, 795–804.

(5) Mannisto, S.; Smith-Warner, S. A.; Spiegelman, D.; Albanes, D.; Anderson, K.; van den Brandt, P. A.; Cerhan, J. R.; Colditz, G.; Feskani, D.; Freudenheim, J. L.; Giovannucci, E.; Goldbohm, R. A.; Graham, S.; Miller, A. B.; Rohan, T. E.; Virtamo, J.; Willett, W. C.; Hunter, D. J. Dietary carotenoids and risk of lung cancer in a pooled analysis of seven cohort studies. *Cancer Epidemiol., Biomarkers Prev.* **2004**, *13*, 40–48.

(6) Ruano-Ravina, A.; Figueiras, A.; Freire-Garabal, M.; Barros-Dios, J. M. Antioxidant vitamins and risk of lung cancer. *Curr. Pharm. Des.* **2006**, *12*, 599–613.

(7) Shukla, Y.; Singh, M. Cancer preventive properties of ginger: a brief review. *Food Chem. Toxicol.* **2007**, *45*, 683–690.

(8) Surh, Y. J.; Lee, E.; Lee, J. M. Chemoprotective properties of some pungent ingredients present in red pepper and ginger. *Mutat. Res.* **1998**, *402*, 259–267.

(9) Baliga, M. S.; Haniadka, R.; Pereira, M. M.; D'Souza, J. J.; Pallaty, P. L.; Bhat, H. P.; Popuri, S. Update on the chemopreventive effects of ginger and its phytochemicals. *Critical Rev. Food Sci. Nutr.* **2011**, *51*, 499–523.

(10) Citronberg, J.; Bostick, R.; Ahearn, T.; Turgeon, D. K.; Ruffin, M. T.; Djuric, Z.; Sen, A.; Brenner, D. E.; Zick, S. M. Effects of ginger supplementation on cell-cycle biomarkers in the normal-appearing colonic mucosa of patients at increased risk for colorectal cancer: results from a pilot, randomized, and controlled trial. *Cancer Prev. Res.* **2013**, *6*, 271–281.

(11) Jolad, S. D.; Lantz, R. C.; Solyom, A. M.; Chen, G. J.; Bates, R. B.; Timmermann, B. N. Fresh organically grown ginger (*Zingiber officinale*): composition and effects on LPS-induced PGE₂ production. *Phytochemistry* **2004**, *65*, 1937–1954.

(12) Sang, S.; Hong, J.; Wu, H.; Liu, J.; Yang, C. S.; Pan, M. H.; Badmaev, V.; Ho, C. T. Increased growth inhibitory effects on human cancer cells and anti-inflammatory potency of shogaols from *Zingiber officinale* relative to gingerols. *J. Agric. Food Chem.* **2009**, *57*, 10645–10650.

(13) Chen, C. Y.; Liu, T. Z.; Liu, Y. W.; Tseng, W. C.; Liu, R. H.; Lu, F. J.; Lin, Y. S.; Kuo, S. H.; Chen, C. H. 6-shogaol (alkanone from ginger) induces apoptotic cell death of human hepatoma p53 mutant Mahlavu subline via an oxidative stress-mediated caspase-dependent mechanism. *J. Agric. Food Chem.* **2007**, *55*, 948–954.

(14) Chen, H.; Soroka, D. N.; Hu, Y.; Chen, X.; Sang, S. Characterization of thiol-conjugated metabolites of ginger components shogaols in mouse and human urine and modulation of the glutathione levels in cancer cells by [6]-shogaol. *Mol. Nutr. Food Res.* **2013**, *57*, 447–458.

(15) Pan, M. H.; Hsieh, M. C.; Kuo, J. M.; Lai, C. S.; Wu, H.; Sang, S.; Ho, C. T. 6-Shogaol induces apoptosis in human colorectal carcinoma cells via ROS production, caspase activation, and GADD 153 expression. *Mol. Nutr. Food Res.* **2008**, *52*, 527–537.

(16) Chen, H.; Lv, L.; Soroka, D.; Warin, R. F.; Parks, T. A.; Hu, Y.; Zhu, Y.; Chen, X.; Sang, S. Metabolism of [6]-shogaol in mice and in cancer cells. *Drug Metab. Dispos.* **2012**, *40*, 742–753.

(17) Hung, J. Y.; Hsu, Y. L.; Li, C. T.; Ko, Y. C.; Ni, W. C.; Huang, M. S.; Kuo, P. L. 6-Shogaol, an active constituent of dietary ginger, induces autophagy by inhibiting the AKT/mTOR pathway in human non-small cell lung cancer A549 cells. *J. Agric. Food Chem.* **2009**, *57*, 9809–9816.

(18) Ishiguro, K.; Ando, T.; Maeda, O.; Ohmiya, N.; Niwa, Y.; Kadomatsu, K.; Goto, H. Ginger ingredients reduce viability of gastric cancer cells via distinct mechanisms. *Biochem. Biophys. Res. Commun.* **2007**, *362*, 218–223.

(19) Gan, F. F.; Nagle, A. A.; Ang, X.; Ho, O. H.; Tan, S. H.; Yang, H.; Chui, W. K.; Chew, E. H. Shogaols at proapoptotic concentrations induce G(2)/M arrest and aberrant mitotic cell death associated with tubulin aggregation. *Apoptosis* **2011**, *16*, 856–867.

(20) Weng, C. J.; Wu, C. F.; Huang, H. W.; Ho, C. T.; Yen, G. C. Anti-invasion effects of 6-shogaol and 6-gingerol, two active

components in ginger, on human hepatocarcinoma cells. *Mol. Nutr. Food Res.* **2010**, *54*, 1618–1627.

(21) Ling, H.; Yang, H.; Tan, S. H.; Chui, W. K.; Chew, E. H. 6-Shogaol, an active constituent of ginger, inhibits breast cancer cell invasion by reducing matrix metalloproteinase-9 expression via blockade of nuclear factor-kappaB activation. *Br. J. Pharmacol.* **2010**, *161*, 1763–1777.

(22) Kim, E. C.; Min, J. K.; Kim, T. Y.; Lee, S. J.; Yang, H. O.; Han, S.; Kim, Y. M.; Kwon, Y. G. [6]-Gingerol, a pungent ingredient of ginger, inhibits angiogenesis in vitro and in vivo. *Biochem. Biophys. Res. Commun.* **2005**, *335*, 300–308.

(23) Hessien, M.; El-Gendy, S.; Donia, T.; Sikkena, M. A. Growth inhibition of human non-small lung cancer cells h460 by green tea and ginger polyphenols. *Anti-Cancer Agents Med. Chem.* **2012**, *12*, 383–390.

(24) Chen, C. Y.; Yang, Y. H.; Kuo, S. Y. Effect of [6]-shogaol on cytosolic Ca²⁺ levels and proliferation in human oral cancer cells (OC2). *J. Nat. Prod.* **2010**, *73*, 1370–1374.

(25) Tan, B. S.; Kang, O.; Mai, C. W.; Tiong, K. H.; Khoo, A. S.; Pichika, M. R.; Bradshaw, T. D.; Leong, C. O. 6-Shogaol inhibits breast and colon cancer cell proliferation through activation of peroxisomal proliferator activated receptor gamma (PPARgamma). *Cancer Lett.* **2013**, *336*, 127–139.

(26) Hu, R.; Zhou, P.; Peng, Y. B.; Xu, X.; Ma, J.; Liu, Q.; Zhang, L.; Wen, X. D.; Qi, L. W.; Gao, N.; Li, P. 6-Shogaol induces apoptosis in human hepatocellular carcinoma cells and exhibits anti-tumor activity in vivo through endoplasmic reticulum stress. *PLoS one* **2012**, *7*, e39664.

(27) Zick, S. M.; Djuric, Z.; Ruffin, M. T.; Litzinger, A. J.; Normolle, D. P.; Alrawi, S.; Feng, M. R.; Brenner, D. E. Pharmacokinetics of 6-gingerol, 8-gingerol, 10-gingerol, and 6-shogaol and conjugate metabolites in healthy human subjects. *Cancer Epidemiol., Biomarkers Prev.* **2008**, *17*, 1930–1936.

(28) Chen, H.; Soroka, D. N.; Zhu, Y.; Hu, Y.; Chen, X.; Sang, S. Cysteine-conjugated metabolite of ginger component [6]-shogaol serves as a carrier of [6]-shogaol in cancer cells and in mice. *Chem. Res. Toxicol.* **2013**, *26*, 976–985.

(29) Zhu, Y.; Warin, R. F.; Soroka, D. N.; Chen, H.; Sang, S. Metabolites of ginger component [6]-shogaol remain bioactive in cancer cells and have low toxicity in normal cells: chemical synthesis and biological evaluation. *PLoS One* **2013**, *8*, e54677.

(30) Mosmann, T. Rapid colorimetric assay for cellular growth and survival: application to proliferation and cytotoxicity assays. *J. Immunol. Methods* **1983**, *65*, 55–63.

(31) Schneider, C. A.; Rasband, W. S.; Eliceiri, K. W. NIH Image to ImageJ: 25 years of image analysis. *Nat. Methods* **2012**, *9*, 671–675.

(32) Collins, T. J. ImageJ for microscopy. *BioTechniques* **2007**, *43*, 25–30.

(33) Ow, Y. P.; Green, D. R.; Hao, Z.; Mak, T. W. Cytochrome c: functions beyond respiration. *Nat. Rev. Mol. Cell Biol.* **2008**, *9*, 532–542.

(34) Walia, V.; Kakar, S.; Elble, R. Micromanagement of the mitochondrial apoptotic pathway by p53. *Front. Biosci.* **2011**, *16*, 749–758.

(35) Guntherberg, H.; Rost, J. The true oxidized glutathione content of red blood cells obtained by new enzymic and paper chromatographic methods. *Anal. Biochem.* **1966**, *15*, 205–210.

(36) Leu, J. I.; Pimkina, J.; Frank, A.; Murphy, M. E.; George, D. L. A small molecule inhibitor of inducible heat shock protein 70. *Mol. Cell* **2009**, *36*, 15–27.

(37) Strom, E.; Sathe, S.; Komarov, P. G.; Chernova, O. B.; Pavlovskaya, I.; Shyshynova, I.; Bosykh, D. A.; Burdelya, L. G.; Macklis, R. M.; Skalter, R.; Komarova, E. A.; Gudkov, A. V. Small-molecule inhibitor of p53 binding to mitochondria protects mice from gamma radiation. *Nat. Chem. Biol.* **2006**, *2*, 474–479.

(38) Nakamura, Y.; Miyoshi, N. Electrophiles in foods: the current status of isothiocyanates and their chemical biology. *Biosci., Biotechnol., Biochem.* **2010**, *74*, 242–255.

(39) Chipuk, J. E.; Maurer, U.; Green, D. R.; Schuler, M. Pharmacologic activation of p53 elicits Bax-dependent apoptosis in the absence of transcription. *Cancer Cell* **2003**, *4*, 371–381.

(40) Vaseva, A. V.; Marchenko, N. D.; Moll, U. M. The transcription-independent mitochondrial p53 program is a major contributor to nutlin-induced apoptosis in tumor cells. *Cell Cycle* **2009**, *8*, 1711–1719.

(41) Nakano, K.; Vousden, K. H. PUMA, a novel proapoptotic gene, is induced by p53. *Mol. Cell* **2001**, *7*, 683–694.

(42) Blagosklonny, M. V. P53: an ubiquitous target of anticancer drugs. *International journal of cancer. J. Int. Cancer* **2002**, *98*, 161–166.

(43) Saito, G.; Swanson, J. A.; Lee, K. D. Drug delivery strategy utilizing conjugation via reversible disulfide linkages: role and site of cellular reducing activities. *Advanced Drug Delivery Rev.* **2003**, *55*, 199–215.

(44) Lyon, R. P.; Meyer, D. L.; Setter, J. R.; Senter, P. D. Conjugation of anticancer drugs through endogenous monoclonal antibody cysteine residues. *Methods Enzymol.* **2012**, *502*, 123–138.